Effect of a Siloxane Moiety on the Anchoring of Ferroelectric Liquid Crystals at the Air−Water Interface†

M. Ibn-Elhaj,*,‡ M. Z. Cherkaoui,§,⊥ R. Zniber,§ and H. Möhwald‡

Max-Planck Institute of Colloids and Interfaces, Rudower chaussee 5, 12489 Berlin, Germany, and Faculty of Science, Mohamed V University, B.P. 1014 R.P. Rabat, Morocco

Received: November 11, 1997; In Final Form: April 20, 1998

We have studied bulk and thin film behavior of a low-molar-mass organosiloxane ferroelectric liquid crystal with a sulfinate as a chiral group. The addition of the siloxane moiety lowers the transition temperature of the bulk smectic phase, increases its thermal stability, and favors a lateral anchoring of the chiral molecules at the air−water interface. The formation of stable monomolecular Langmuir films of this LMM ferroelectric liquid crystal permits the control of the molecular orientation via lateral density changes, and consequently in-situ investigations of the interfacial ordering and orientation. Uniform mono- and multilayer films with well-defined orientation can be transferred onto solid substrate for further studies.

I. Introduction

Chiral low-molar-mass (LMM) smectogens exhibiting S_{C^*} phases have been studied extensively because of their ferroelectric properties[1,2] and their possible applications such as light valves,[3] displays,[4] spatial light modulators,[5] and pyroelectric detectors.[6] Although each layer possesses an effective polarization, the bulk polarization can be observed only by unwinding the macroscopic helical arrangement along the layer normal. This can be achieved by surface effects such as with surface-stabilized ferroelectic liquid crystals (SSFLC).[3] However, difficulties in forming uniform films with thicknesses in the range of microns hinder the exploitation of SSFLC during the orientation process. Thus, besides a fundamental interest, understanding the anchoring of ferroelectric liquid crystals is of crucial importance for the construction of efficient LCD displays. Furthermore, requirements, such as a wide S_{C^*} temperature range around room temperature and a large spontaneous polarization, Ps, which generally leads to a short response time, for these materials to be applicable to the development of electrooptical devices are still considered of a fundamental interest.[7]

Previous studies have shown that the presence of an additional siloxane group lowers the transition temperature and enhances the mechanical properties of the smectic phase.[8−10] This is due to the siloxane moieties, which are incompatible with the rest of the molecule;[9] consequently, they locate themselves in separate sublayers resembling the case of a side-chain liquid crystalline polymer where the backbones are inserted between the smectic layers. In addition, recent studies[11−13] have shown that a chiral sulfinate group directly attached to the rigid core of the molecule leads to material with high Ps. This is due to its highly polarized S═O bond which induces a large dipole moment component transverse to the molecular tilt plane.[13]

TABLE 1: Bulk Polymorphism of the 12-BTS−O11-Me and the Corresponding Siloxane Derivative 12-BTS−O11-silo

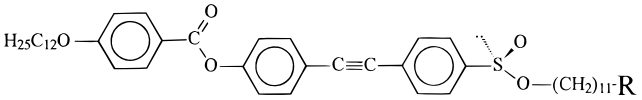

compound	R	polymorphism
12-BTS−O11-Me	$-CH_3$	K $\xrightarrow{86\ °C}$ SmC* $\xleftrightarrow{103\ °C}$ SmA $\xleftrightarrow{108.5\ °C}$ I
12-BTS−O11−Silo	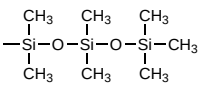	K $\xrightarrow{60\ °C}$ SmC* $\xleftrightarrow{100\ °C}$ I

On the basis of the results above, we have synthesized a new ferroelectric liquid crystal with the sulfinate as the chiral group plus an additional siloxane moiety as the endgroup in order to obtain both low-temperature SmC* and high Ps. Detailed studies of the bulk behavior by systematically varying the size and the position of the siloxane part are currently being performed and will be published soon.[14] In the present paper, we will present an analysis of the Langmuir film behavior at the air−water interface and a comparison of such behavior to the bulk behavior of a chiral sulfinate siloxane molecule denoted 12-BTS−O11-silo (see Table 1). The effects of the additional Hexamethyltrisiloxane (HMTS) part on two- and three-dimensional behavior have been determined by systematically comparing such behavior to the behavior of the corresponding chiral sulfinate homologous 12-BTS−O11-Me (Table 1) without the siloxane moiety.[12,15] We particularly show that the existence of a siloxane endgroup favors a monomolecular Langmuir film formation at the air−water interface. The molecular orientation within the film can be controlled via lateral density changes in the Langmuir trough. The interfacial ordering is investigated, and uniform films with specific molecular orientation can be transferred onto solid substrate for further analysis.

II. Experimental Section

The preparation of the sulfinate 12-BTS−O11-silo involves asymmetric synthesis of undec-(10-enyl)-4-bromobenzenesul-

* Corresponding author.

† PACS. 68.18.+p: Langmuir−Blodgett films. PACS. 64.70.Md: transitions in liquid crystals. PACS. 61.30.Gd: orientational order of liquid crystals. PACS. 77.84.Nh: ferroelectricity in liquid crystals.

‡ Max-Plank Institute of Colloids and Interfaces.

§ Faculty of Science.

⊥ Permanent address: ROLIC Research LTD, Gewubestrasse 18, CH-4123 Allschwil, Switzerland.

S1089-5647(98)00153-9 CCC: $15.00
Published on Web 06/12/1998

finate,[12] followed by a platinum complex (platinum divinyltetramethyldisiloxane) addition reaction of heptamethyltrisiloxane. The undec-[10-(1,1,3,3,5,5,5-heptamethyl)trisiloxanyl]-4-bromobenzenesulfinate obtained is catalytically coupled to an ethynyl mesogenic rest using a modified Heck catalytic coupling procedure. Further details will be given elsewhere.[14]

X-ray diffraction studies on bulk materials were carried out with a Guinier type chamber described in ref 9.

The pressure−area isotherms were recorded with a commercial automatic Lauda film balance. The temperature and the pressure of the Langmuir trough were controlled to an accuracy of ±0.2 °C and ±0.2 mN m^{-1}. The monolayers were spread on pure water (Millipore, 18.2 M Ω cm) from chloroform solutions (1 mM). The compounds and their spread monolayers were insoluble in water.

Silicon wafers with naturally grown oxide layers were used as solid substrates. The floating films were transferred onto the SiO_2 surface, made hydrophilic, at 3.5 and 10 mN m^{-1} at a dipping speed of 2 mm/min. Specular X-ray scattering of the transferred films was performed with a commercial $\theta/2\theta$ instrument (STOE & CIE GmbH Darmstadt, $U = 40$ kV, $I = 50$ mA, $\lambda = 1.54$ Å (Cu Kα)). The divergence of the incoming beam was 0.1°; the 2θ resolution was 0.05°.

The Brewster angle microscope (BAM, NFT Göttingen) was mounted on a Langmuir film balance from R&K (Wiesbaden, D). The spacial resolution of the method is about 4 μm. Experimental details of the BAM are described elsewhere.[16]

Surface potential measurements were performed with a vibrating plate, from KSV (Helsinki), mounted on a large Langmuir film balance from R&K, to obtain a high compression ratio. This allows measurement in the whole isotherm range under equilibrium conditions. The accuracy of the method is of about ± 5 mV.

III. Results and Discussions

III.1. Bulk Phase Behavior and Structure. The bulk thermotropic polymorphism of 12-BTS−O11-silo was studied by differential scanning calorimetry (DSC) and classical polarizing optical microscopy. The textures observed suggest the presence of a smectic C (or C*) mesophase. The tilted nature of the smectic mesophase was confirmed by optical microscopy on free-standing thin films which exhibit typical schlieren textures characteristic of a smectic C mesophase.[8] Table 1 summarizes the polymorphism of 12-BTS−O11-silo smectogen obtained together with the one of the 12-BTS−O11-Me smectogen, previously determined.[12,15] The latter shows both a ferroelectric SmC* phase and a SmA phase. However, the corresponding siloxane homologue 12-BTS−O11-silo shows only a SmC* phase. The suppression of the SmA phase is due to the bulky siloxane unit which has a large cross-sectional area and consequently imposes a high and constant tilt of the aromatic core [see also ref 8] contrary to 12-BTS−O11-Me whose tilt is smaller (Table 2) and decreases continuously with increasing the temperature and finally disappears into the SmA phase.[15]

The X-ray diffraction patterns of 12-BTS−O11-silo (Figure 1) are in perfect accordance with the optical observations. They contain, in the whole temperature range 60−100 °C, two equidistant sharp Bragg reflections in the small-angle region, indicative of the smectic layering. In the wide-angle region, they contain a diffuse band (B) at about 4.6 Å, corresponding to the liquid-like conformation of the paraffin chains and to the lateral correlation of the aromatic cores, and one less diffuse band (A) at about 7 Å, corresponding to the liquid-like arrangement of the siloxane groups.

TABLE 2: Smectic Period (d), Molecular Lengths (L), the Deduced Molar Volumes (V), the Calculated Area Occupied in the Smectic Planes by Two Molecules ($S = 2V/d$), and the Tilt Angle, θ, of the Aromatic Cores (Calculated Using the Equation $\arccos(2\sigma_{Ar}/S)$)

compound	d/Å	L/Å	V/Å^3	S/Å^2	θ/deg
12-BTS−O11-Me	44.5[a]	'48'	1100 ± 100	49	22[b]
12-BTS−O11-silo	52	55	1500 ± 100	58	38

[a] Corresponds to the maximum value measured in the SmA phase.[12] [b] Corresponds to the maximum tilt angle in the SmC* phase (i.e., at 85 °C).

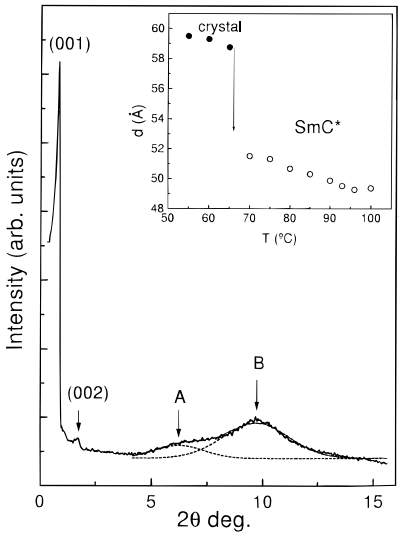

Figure 1. Typical X-ray diffraction pattern of the smectic C* phase of 12-BTS−O11-silo at 70 °C: contain two sharp Bragg reflections, (001) and (002), in the small angle region, corresponding to the smectic layering. In the wide-angle region they contain two diffuse bands at (B) 4.6 Å and (A) 7 Å (A) corresponding to liquidlike conformation of the paraffin and the siloxane parts, respectively. The dashed lines represent a fit using a double Gaussian function. The inset represents the variation of the smectic period, reflection (001), as a function of temperature.

Concerning the ferroelectric properties, a spontaneous polarization of about 82 nC/cm^2 was measured at a temperature of about 80 °C by applying an electric field of ±17.5 V perpendicular to the plates of a 4 μm SSFLC cell (E. H. C. Company, Ltd., Tokyo). This value is close to that of 12-BTS−O11-Me.[15] The tilt angle, defined as the half-angle between two extreme optical states corresponding to the two polarities of the applied electric field, was measured as a function of temperature by application of about 0.1 Hz frequency wave rectangular voltage. Its value of about 41° is independent of the temperature and the applied voltage.

The smectic period (see inset in Figure 1) is slightly decreasing (about 5%) with the temperature. This unusual effect is not due to any change of the tilt angle of the aromatic parts. Indeed, the later is determined to be constant with the temperature using electrooptical measurements. The origin of this phenomenon, already observed with other ferroelectric three-block smectogens,[8,17] is probably due to the bilayering of the siloxane parts which decreases $d_{siloxane}$ through their lateral expansion with the temperature (see below). The mesophase of 12-BTS−O11-silo is clearly smectic C* in nature, although the value of the smectic period is of about one molecular length. This unexpected phenomenon has been observed with other organosiloxane ferroelectric molecules[8] and is due to the presence of the bulky siloxane part. The three-dimensional bulk structure of the smectic C* phase of 12-BTS−O11-silo is

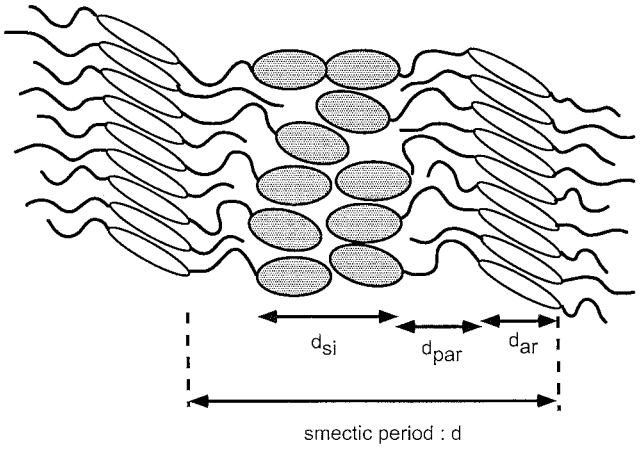

Figure 2. Schematic representation of the smectic C bilayer of 12-BTS−O11-silo compound. The central part of the smectic layer is arbitrary chosen to be formed of the siloxane sublayers (the HMTS groups are represented with the filled ellipses). This part is fringed with the disordered paraffin chains (waxy lines) arranged in single layers. The aromatic cores (elongated ellipses) are located within distinct sublayers in monolayered arrangement and tilted with respect to the normal layers.

presumably similar to the one proposed earlier.[8] This structure consists of successive superposition of paraffin, aromatic, and siloxane sublayers due to their tendency to segregate as schematically illustrated in Figure 2. The smectic period results from the contribution of the three sublayer thicknesses ($d = 2d_{\text{paraffin}} + d_{\text{aromatic}} + d_{\text{siloxane}}$). Since the aliphatic tails are in a disordered conformation, the smectic period obtained ($d \cong L$) results mainly from the balance between the tilt of the aromatic cores, decreasing d_{aromatic}, and consequently, d, and the bilayering of the siloxane parts which, however, increases d. In the present case these two effects compensate each other. Additionally, a tilt of the rather long HMTS siloxane group may also exist and thus contributes to the decrease of d_{siloxane}. Indeed, investigations of Langmuir monolayers of cyanobiphenyl compounds, terminated with the HMTS siloxane moiety, indicate that this part is tilted with respect to the water surface.[18]

The molecular structure proposed (Figure 2) can be discussed in terms of the calculated molecular area S using the molar volume of the molecule (see Table 2), estimated with the usual assumption of additivity of the partial molar volumes of the constituent parts of the molecules ($V = V_{\text{paraffin}} + V_{\text{aromatic}} + V_{\text{siloxane}}$) using the available volume data ($V_{CH_2} \cong 28$ Å^3 and $V_{CH_3} \cong 50$ Å^3,[19] V(aromatic part of n-BTS−Om) $\cong 390$ Å^{-3} [15] and $V_{\text{siloxane}} \cong 400$ Å^3 [refs 8−9 and references cited therein]. Because of the mutual incompatibility of the three constituent parts, the molecules must pile up in layers pointing up and down (Figure 2). As a result of the two-sided symmetry of the smectic layers, the molecular area ($S = 2V/d \cong 58 \pm 4$ Å^2) corresponds to the area in the smectic planes occupied by two molecules. This value suggests the following comments regarding the molecular packing in each one of the three sublayers of the smectic C* structure (Figure 2). Concerning the aromatic sublayer, the S value is larger than twice the molecular area of the aromatic cores ($\sigma_{\text{ar}} \cong 23$ Å^2 [19]). Clearly, this suggests a monolayered arrangement of tilted aromatic cores, with a tilt angle of about $\arccos(2\sigma_{\text{ar}}/S) \cong 38 \pm 5$ °. This is in good agreement with the value of the tilt angle measured optically. Concerning the siloxane sublayers, the S value is intermediate between one and two times the cross area of the siloxane moiety ($\sigma_{\text{si}} \cong 45$ Å^2 [20]) in its bulk liquid phase. This suggests a partially bilayered arrangement of the siloxane endgroups, with a degree

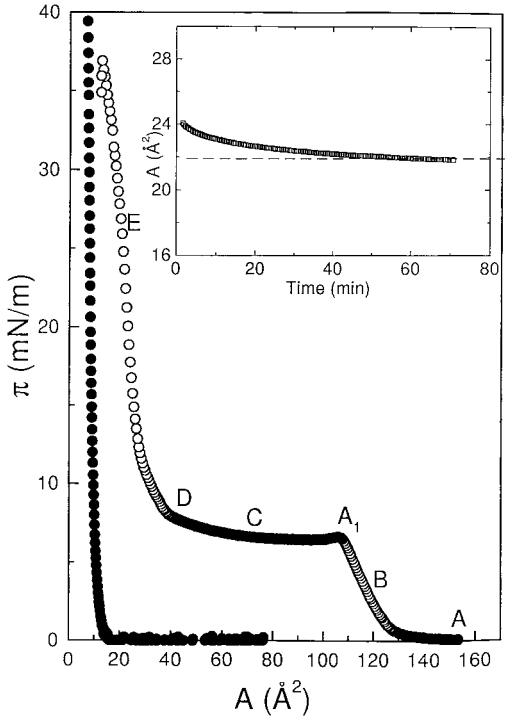

Figure 3. The measured $\pi-A$ curves at the air−water interface at 20 °C for 12-BTS−O11-silo (open circles) and 12-BTS−O11-Me (filled circles); the inset represent the relaxation curve (isobar) of 12-BTS−O11-silo Langmuir film measured at 20 mN m^{-1}.

of bilayering ($\tau = 2 - S/\sigma_{\text{si}}$ [ref 8 and references therein]) of about 0.7. Finally, concerning the paraffin sublayers, the S value is in agreement with what is known of the lateral expansion of paraffin chains in a disordered conformation and is therefore consistent with the single layered arrangement proposed in Figure 2.

III.2. Interfacial Phase Behavior and Structure. Figure 3 shows the typical pressure−area isotherms obtained for 12-BTS−O11-silo and 12-BTS−O11-Me at the air−water interface. The $\pi-A$ diagram of 12-BTS−O11-Me indicates that no defined monolayer is formed and that no collapse point could be observed. There is a sharp increase of the surface pressure at an apparent area per molecule too small for even the densest packing of the molecules in a monolayer, and whose value depends on spreading conditions. The absence of Langmuir monolayers is probably due to the stiffness of the molecules and large intermolecular interactions which prevent the spreading of single molecules. The compound 12-BTS−O11-silo, however, allows Langmuir monolayer formation. This clearly means that the siloxane endgroup decreases the intermolecular interactions and favors the anchoring of the molecule to the water surface. At this stage a question arises quite naturally: why is the anchoring favored with the presence of the siloxane? The answer to this question is probably related to the unique property of the silicones with respect to their interfacial activity compared to hydrocarbons and fluorocarbons. The silicones do not fit the simple pattern that a reduction in surface energy means an increase in hydrophobicity and thus the interfacial tension relative to water.[21] Indeed, from the surface tension point of view, the order of increasing surface activity is flurocarbons−silicones−hydrocabons. However, from the viewpoint of the interface against water, the order of increasing surface activity is fluocarbons−hydrocabons−silicones.[21] The large activity of the siloxane toward the water surface is attributed to the flexibility of the siloxane part, which can adopt

an orientation involving interaction with the water phase giving rise to a relatively low interfacial tension relative to water.[21] It was found that poly(dimethylsiloxane) (PDMS) adopts a configuration such that all the Si−O bonds can be aligned with the water surface. The driving force for this highly ordered configuration was ascribed to the polar interactions between the Si−O bonds, found to be 50% ionic, and the water.[21]

The $\pi-A$ isotherm obtained contains different regions corresponding to different phases. In the monolayer phase the area per molecule values range between 110 and 137 Å^2. These are large molecular areas, and they clearly indicate that the molecules lie parallel to the water surface. This planar anchoring favored by the siloxane group is probably also due to the presence of a strong lateral dipole moment in the molecule, which should be oriented toward the water surface. When the monolayer is compressed beyond the closest packing of the horizontally oriented molecule, a phase transition occurs (at A_1). This probably corresponds to the expulsion of one molecular end out of the water as usually observed at the air−water interface with molecules containing two hydrophilic headgroups.[22,23] On further compression beyond the monolayer collapse point at A_1, first a plateau is observed and then the pressure increases slowly starting at an area of about 60 Å^2 and then more steeply reach a value of about 35 mN m^{-1} at small areas when the film has collapsed to the bulk crystalline phase. The change in the molecular orientation from planar, at large areas per molecule, to vertical one, at small areas per molecule, seems to be consistent with the value of the interfacial energy, $\pi_1 = 6.7$ mN m^{-1}, at the transition point A_1. The latter is close to the energy corresponding to the difference in the adhesion energy between parallel and perpendicular orientation for some mesogens, which is of about 6 mN m^{-1}.[24]

Using Brewster angle microscopy information on the lateral film homogeneity and phase transitions were obtained. The monolayer (see Figure 4A,B) is completely homogeneous at least on a mesoscopic length scale, since no anisotropy was detected when rotating the analyzer. After the collapse of the monolayer at A_1, one observes spots due to the nucleation of the new phase (Figure 4C). With further compression, these domains fill progressively the space (Figure 4D) and crystallization of the film occurs as attested with the cracks observed when expanding the film (Figure 4E), and the nonreversibility of the isotherm at 20 °C usually observed when the bulk is in the crystalline state.[25] This can be avoided by heating the film to a temperature of about 50 °C. Then, a helical arrangement of the molecules appears due to the chirality of the molecules (Figure 4F); domains with different brightnesses are observed in which molecules possess different azimuthal orientations as attested when rotating the analyzer.

X-ray reflectivity measurements were performed on films transferred on SiO_2 solid substrates at 3.5 and 10 mN m^{-1}. The X-ray reflectograms obtained (Figure 5) show pronounced maxima and minima indicating good thickness uniformity**.** At this stage we only deduce the thicknesses, $d_1 \cong 14 \pm 1$ Å at 3.5 mN m^{-1} and $d_2 \cong 74 \pm 1$ Å at 10 mN m^{-1}. These are derived from the minima in the reflectivity curves without any fitting procedure.[25] Detailed investigations of the microscopic structure and orientation are necessary and will soon be performed using X-ray reflectivity and diffraction directly at the air−water interface. However, the thickness measurements confirm, at least qualitatively, the interpretations above. The film transferred at 3.5 mN m^{-1} consists of a monolayer, since d_1 times the corresponding area $A_{L1} \cong 115 \pm 1$ Å^2 is nearly equal to the volume of a single molecule (see Table 2).

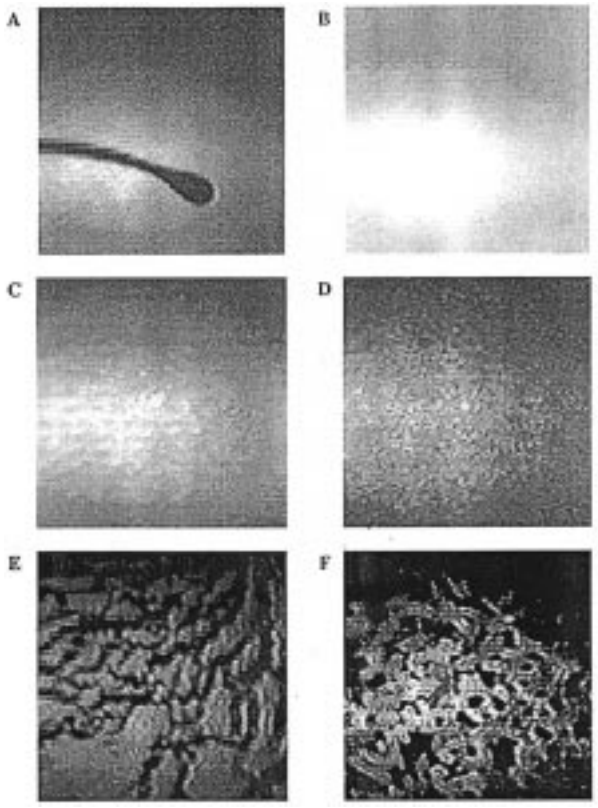

Figure 4. Brewster angle microscopy textures of 12-BTS−O11-silo. Images A−E indicated in the isotherm (Figure 3) have been taken at 20 °C. The image F has been taken at a temperature of about 50 °C and a pressure of about 20 mN m^{-1}.

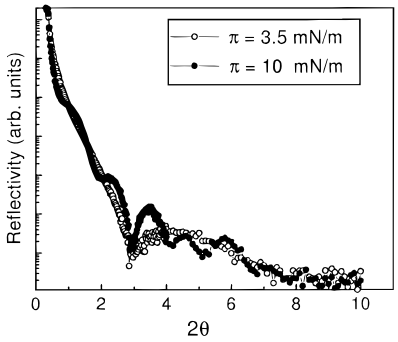

Figure 5. X-ray reflectivity curves of films transferred onto SiO_2 substrate (a) at $\pi \cong 3.5$ mN m and (b) at $\pi \cong 10$ mN m^{-1}.

Furthermore, the thickness d_1 is well below that expected for the stretched molecule oriented normally to the surface (Table 2). Assuming rodlike molecules the tilt angle in the monolayer can be roughly estimated according to $\theta_{L1} = \arccos(d_1/L) \cong 75 \pm 1°$. This means that the molecules in the monolayer have a planar anchoring with a small tilt angle from the water surface of about 15°. The thickness $d_2 \cong 74 \pm 1$ Å is larger than one molecular length, and clearly indicates that the film transferred at 10 mN m^{-1} contains at least two molecules (bilayer). The bilayer formation seems to be consistent with the surface potential measurements as will be discussed in the next section. To obtain further details on the molecular ordering and structure, we are currently performing SHG measurements and are also planning to do in-plane X-ray diffraction at the air−water interface (using synchrotron radiation) soon.

III.3. Interfacial Polar Ordering. The polar ordering within the film and the related phase transitions were probed with surface potential measurements directly at the air−water

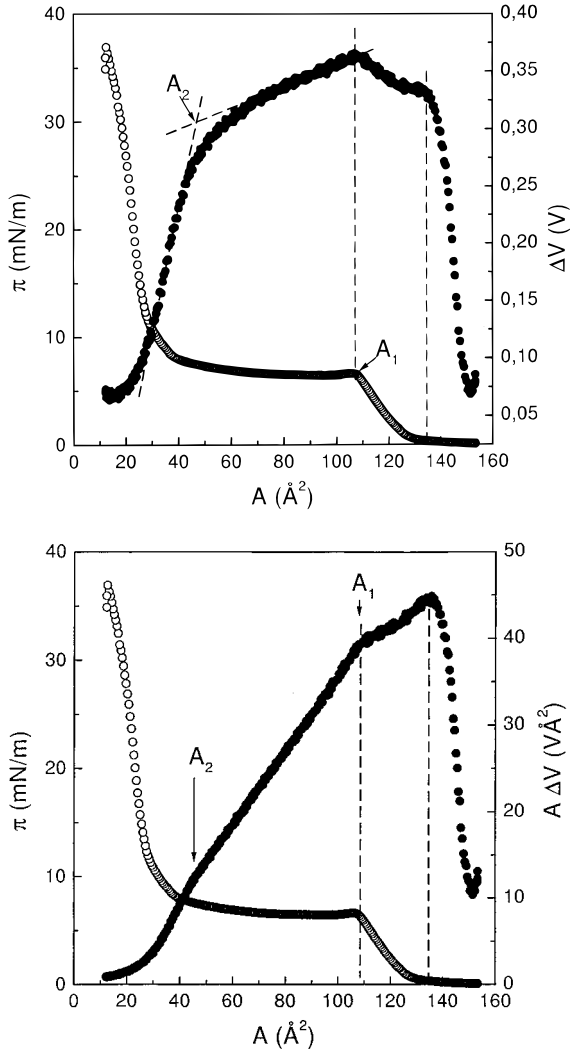

Figure 6. (a) $\pi-A$ isotherm of 12-BTS−O11-silo (open circles), together with the simultaneously measured surface potential (closed circles), and (b) $\pi-A$ isotherm of 12-BTS−O11-silo (open circles) together with the calculated A ΔV (closed circles).

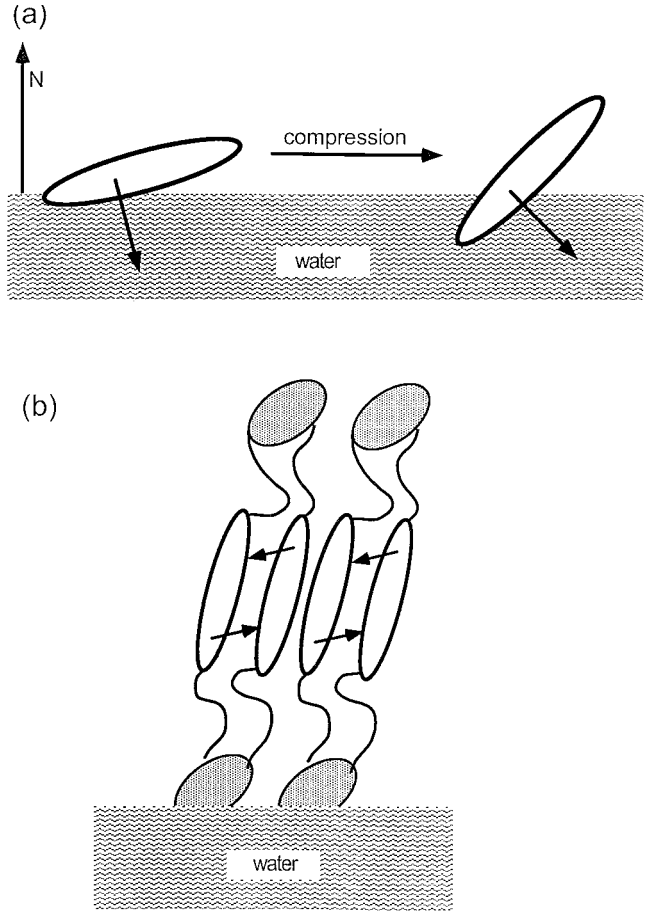

Figure 7. Schematic representation of (a) the molecular reorientation during the compression of the monolayer and (b) a possible molecular arrangement of within the bilayer film at the air−water interface.

interface at 20 °C. Figure 6a shows the simultaneously measured surface potential and surface pressure. The surface potential first rises monotonically from zero at large areas per molecule, to about 325 mV at an area $A \cong 137$ Å^2 when the monolayer is completely closed. During the compression of the monolayer ΔV rises slowly to $\Delta V_1 \cong 360$ mV at the transition point A_1 where a kink occurs in the surface potential as it does in the surface pressure. On further compression, ΔV decreases slowly to $\Delta V_2 \cong 300$ mV at an area $A_2 \cong 44$ Å^2, defined by the inflection point, where the surface potential changes its slope and decreases more steeply to $\Delta V \cong 70$ mV at small areas. This inflection point at A_2 may corresponds to a second-order phase transition with the formation of a bilayer as sketched in Figure 7b. The value A_2 is close to the cross sectional area of the siloxane group (≅ 45 Å^2 [20]) and indicates that this transition occurs when the molecules have the closest possible packing allowed by the bulkier siloxane part, as usually observed with organosiloxane mesogens.[18,25] The formation of a bilayer such as that sketched in Figure 7b is consistent with the drop of the surface potential at A_2. Indeed, this arrangement the lateral dipole moment becomes nearly parallel to the water surface and consequently has negligible contribution to ΔV. Furthermore, knowing the thickness, $d_2 \cong 74$ Å, of the films transferred above 8 mN m^{-1} (i.e., below A_2), one obtains at these pressures a total volume of $d_2A_2 \cong 3256$ Å^3. This is nearly equal to the volume occupied by two molecules. Finally, it is interesting to note that d_2 is significantly bigger than the bulk smectic period (≅52 Å), indicating a different internal bilayer structure probably with a smaller tilt angle with respect to the water normal, either due to some surface field effects and/or to the lateral compression of the film.

For quantitative interpretation and discussion of the result we use the Helmholtz equation (HE) for un-ionized molecules. This equation is derived by analogy between the monolayer and a parallel-plate capacitor.[26] It relates the surface potential ΔV for a surface covered with dipoles, defined as the difference in potential between the film-covered surface and a clean water surface, to an average dipole moment for the monolayer-forming molecules according to

$$\Delta V = \rho\mu_\perp/\epsilon_r\epsilon_0 \qquad (1)$$

where ϵ_r is the relative permittivity of the monolayer, $\epsilon_0 = 8.85 \times 10^{-12}$ C(V m)$^{-1}$ is the permittivity of the free space, $\rho = 1/A$ is the surface density of the dipoles (A is the average area per molecule), and $\mu_\perp = \mu \cos(\theta)$ is the average dipole moment normal to the surface. Thus ΔV depends on both the packing density ρ and the orientation of the molecules in the monolayer θ. Using the HE, one can discuss the data obtained in terms of the parameter $A\Delta V$, which should be proportional to the vertical component of the average dipole moment within the film. In the monolayer region, ΔVA decreases slightly (from ≅45 to ≅40 V Å^2) during compression of the monolayer (see Figure 6b).

This means that the vertical component of the effective dipole moment $\mu_\perp$ decreases during compression, and consequently the molecules change their orientation θ. This can be understood keeping in mind that the chiral molecule present possesses a strong lateral dipole moment.[13] Since the molecules are laterally anchored to the water surface, this lateral dipole gives rise to the main contribution of the measured surface potential. The observed decreases of ΔVA indicate a decrease of the vertical component of the lateral dipole moment. Consequently, the tilt angle of the molecules with respect to the water normal becomes smaller, and thus the molecules tend to stand up under compression as schematically illustrated in Figure 7a. Furthermore, the transition to a second phase at the area A_2 is consistent with the observed behavior of ΔVA which vary linearly between A_1 and A_2 as expected for a two phase coexistence region [see ref 27]. Deviations from the linearity start at the transition area A_2.

Since the polarization is defined as the dipole moment per unit volume, the component of the polarization normal to the interface $P_\perp$ can be given by

$$P_\perp = \mu_\perp / V = \epsilon_r \epsilon_0 \Delta V / d \qquad (2)$$

where A is the molecular area, d the film thickness, and $V = Ad$ is the total volume. Using the values of d_1, ΔV_1, and $\epsilon_r = 3$, the polarization of the monolayer (i.e., the polarization of a laterally anchored molecule) is $P_{\perp,1} \cong 663$ nC cm^{-2}.

Since the bulk spontaneous polarization is defined as $\mathrm{Ps} = f\, n_b\, \mu_T$,[28] where μ_T is the transverse molecular dipole, n_b the number of molecules per unit volume, and f a yield factor. This parameter generally ranges from 10^{-3} to 10^{-1} and is a direct measure of the molecular rotation around the long axis.[28] We can then calculate for this molecule a yield factor, defined as $P_S/P_{\perp,1}$, of about 0.16, using the measured spontaneous polarization of the bulk SmC* phase (Ps $\cong$ 82 nC cm^{-2}). This is excellent agreement with the result of ref 13.

IV. Conclusion

In this paper we presented two- and three-dimensional behavior of a new organosiloxane ferroelectric liquid crystal with the sulfinate as a chiral group. The use of a bulky siloxane moiety decreases the intermolecular interactions. This lowers the bulk transition temperature without any decrease of the spontaneous polarization and permits a lateral anchoring of the molecules onto the polar water surface. Uniform monomolecular films of this ferroelectric liquid crystal can be obtained at the air−water interface and transferred onto various solid substrates. Consequently, these films can be used as model systems to understand the interfacial interactions involved and then the design of efficient surface stabilizing ferroelectric liquid crystals by an appropriate choice of the molecules and surfaces. Systematic studies (both the microscopic molecular ordering and orientation) on the anchoring of various organosiloxane molecules and substrates are currently being performed with the help of other methods such as SHG, X-ray diffraction, and AFM.

Acknowledgment. The authors thank Drs. D. Guillon and A. Skoulios for X-ray diffraction facilities and S. Paus, T. Fuherer, and Prof. Heppke for the electrooptical measurement in the bulk SmC* phase of 12-BTS-O11-Silo smectogen.

References and Notes

(1) Meyer, R. B.; Liébert, L.; Strzelecki, L.; Keller, P. *J. Phys. Lett.* **1977**, *36*, L69.
(2) Martinot-Lagarde, Ph. *J. Phys. Lett.* **1977**, *38*, 17.
(3) Clark, N. A.; Lagerwall, S. T. *Appl. Phys. Lett.* **1980**, *36*, 899; *Ferroelectrics*, **1984**, *59*, 25.
(4) Patel, J. S.; Goodby, J. W.; Leslie, T. M. *Proc. SPIE* **1986**, *613*, 130.
(5) Armitage, D.; Thakara, J. I.; Clark, N. A.; Handschy, M. A. *Proc. SPIE* **1986**, *684*, 60.
(6) Glass, A. M.; Patel, J. S.; Goodby, J. W.; Olson, D. H.; Geary, J. M. *J. Appl. Phys.* **1986**, *60*, 2778.
(7) Goodby, J. W.; Blinc, R.; Clark, N. A.; Lagerwall, S. T.; Osipov, M. A.; Pikin, S. A.; Sakurai, T.; Yoshino, K.; Zeks, B.; *Ferroelectric Liquid Crystals; Principles, Properties, and Applications*; Gordon and Breach Science Publishers: New York, 1991.
(8) Ibn-Elhaj, M.; Skoulios, A.; Guillon, D.; Newton, J.; Hodge, P.; Coles, H. J. *J. Phys. II Fr.* **1996**, *6*, 271.
(9) Ibn-Elhaj, M.; Coles, H. J.; Guillon, D.; Skoulios, A. *J. Phys. II Fr.* **1993**, *3*, 1807.
(10) Coles, H.; Owen, H.; Newton, J.; Hodge, P. *Liq. Cryst.* **1993**, *15*, 739.
(11) Soldera, A.; Nicoud, J.-F.; Galerne, Y.; Skoulios, A.; Guillon, D.; *Chem. Mater.* **1994**, *6*, 625.
(12) Cherkaoui, M. Z.; Nicoud, J.-F.; Guillon, D.; *Chem. Mater*. **1994**, *6*, 2026.
(13) Cherkaoui, M. Z.; Nicoud, J.-F.; Galerne, Y.; Guillon, D. *J. Chem. Phys.* **1997,** *106*, 7816.
(14) Cherkaoui, M. Z.; Zniber, R.; Mery, S.; Nicoud, J.-F.; Guillon, D.; Ibn-Elhaj, M., To be published.
(15) Cherkaoui, M. Z. Ph.D. Thesis, Univeristé Louis Pasteur de Strasbourg, France, 1993.
(16) Honig, D.; Möbius, D. *J. Phys. Chem.* **1991**, *95*, 2092−2097. Honig, D.; Overbeck, G. A.; Möbius, D. *Adv. Mater.* **1991**, *4*, 419−424.
(17) Newton, J.; Coles, H. J.; Hywel, H.; Hodge, P. *Ferroelectrics*, **1993**, *148*, 379.
(18) Ibn-Elhaj, M.; Möhwald, H.; Cherkaoui, M. Z.; Zniber, R. *Langmuir* **1998**, *14*, 504−516.
(19) For example, see: Guillon, D.; Skoulios, A.; Benattar, J. J. *J. Phys. Fr.* **1986**, *47*, 133.
(20) Schmaucks, G.; Sonnek, G.; Wustneck, R.; Herbst, H.; Ramm, M. *Langmuir*, **1992**, *8*, 1724. Boyer, R. F.; Miller, R. L. *Rubber Chem. Technol*. **1978**, *51*, 718;.
(21) See: Owen, M. J. *Ind. Eng. Chem. Prod. Res. Dev.* **1980**, *19*, 97−103 and refs cited therein.
(22) Kellner, B. M. J.,; Cadenhead, D. A. *J. Colloid Interface Sci.* **1978**, *63*, 452.
(23) Zhang, T.; Feng, Z.; Wong, G. W.; Ketterson, J. B. *Langmuir*, **1996**, *12*, 2298.
(24) For example, see Cognard, J. *Alignment of Nematic Liquid Crystals and their Mixtures*; Gordon Breach: London, 1982.
(25) Ibn-Elhaj, M.; Riegler, H.; Möhwald, H. *J. Phys. I Fr.* **1996,** *6*, 969.
(26) Helmholtz, H., abhandlungen zur Thermodynamik Chemischer Vorgange; Herausgegeben von Dr, Max-Planck: Leipzig, 1902; pp 51−83.
(27) Miller, A.; Helm, C. A.; Möhwald, H., *J. Phys. Fr.* **1987**, *48*, 969.
(28) de Gennes, P. G.; Prost, J. *The Physics of Liquid Crytals*, 2nd ed.; Clarendon: Oxford, 1993.